JOC Article
pubs.acs.org/joc

Self-Assembly of C_3-Symmetrical Hexaaryltriindoles Driven by Solvophobic and CH$-\pi$ Interactions

Eva M. García-Frutos,[†] Gunther Hennrich,[‡] Enrique Gutierrez,[†] Angeles Monge,[†] and Berta Gómez-Lor*,[†]

[†]*Instituto de Ciencia de Materiales de Madrid, CSIC, Cantoblanco, 28049 Madrid, Spain and* [‡]*Departamento de Química Orgánica, Universidad Autónoma de Madrid, 28049 Madrid, Spain*

bgl@icmm.csic.es

Received September 17, 2009

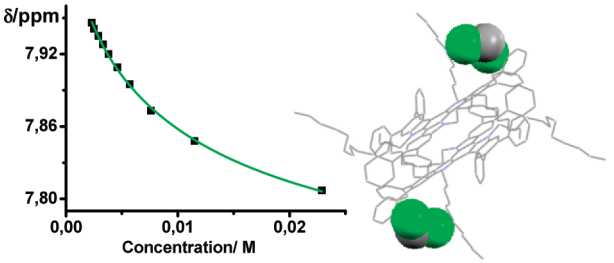

The synthesis and aggregation properties of a series of differently substituted star-shaped hexaaryltriindoles both in solution and in the solid state are being reported. While these molecules do not show any significant intermolecular aggregation in $CDCl_3$, it has been possible to induce aggregation by increasing the polarity of the solvent and therefore facilitating the occurrence of solvophobic forces. A study of the influence of the electronic character of peripheral substituents on the self-association behavior in solution has shown that increasing the electron-donor character of the substituents facilitates self-association while derivatives substituted with electron-acceptor substituents do not self-assemble. The electronic nature of the substituents also has an influence in the geometry of the stacking of these derivatives observed in the solid state. While unsubstituted hexaphenyl triindole self-assemble in a staggered face-to-face arrangement, attaching six cyano functional groups results in an offset stacking. The influence of the substituents in the strength and geometry of the stacking tendency contrasts with the trend expected for an aggregation induced solely by $\pi-\pi$ interactions, but can be explained considering an important contribution of multiple cooperative CH$-\pi$ interactions.

Introduction

Intermolecular interactions involving aromatic rings are of primary importance in biochemistry and supramolecular and materials chemistry.[1] Important processes such as protein−ligand recognition, host−guest binding, or the self-assembly of organized nanostructures are the result of the interplay of different weak interactions[2] such as $\pi-\pi$ stacking and XH$-\pi$ (X = O, N, C) or cation$-\pi$ interactions.

In spite of their importance both in synthetic and natural events, the study of these interactions is usually difficult due to their weak nature and their cooperative occurrence that complicate their individual study. The influence of the electronic nature of substituents attached to the aromatic units on the association processes has been systematically analyzed in order to shed light on the intrinsic nature of these interactions, but sometimes the effect exerted by the substituents in the strength of the different interactions follows opposed trends and therefore conclusions have to be drawn with caution.

For example, $\pi-\pi$ stacking is usually favored by attachment of electron-withdrawing substituents to the aromatic surfaces[3] as a consequence of the decrease of a repulsive

*To whom correspondence should be addressed. Phone: (+34) 91-3349031. Fax: (+34) 91-3720623.

(1) Meyer, E. A.; Castellano, R. K.; Diederich, F. *Angew. Chem., Int. Ed.* **2003**, *42*, 1210–1250.

(2) Steed, J. W.; Atwood, J. L. *Supramolecular Chemistry*; John Wiley and Sons: Chichester, UK, 2009.

(3) Several models have been designed to quantify the influence of the substituents on the stacking: (a) Cockroft, S. L.; Perkins, J.; Zonta, C.; Adams, H.; Spey, S. E.; Low, C. M. R.; Vinter, J. G.; Lawson, K. R.; Urch, C. J.; Hunter, C. A. *Org. Biomol. Chem.* **2007**, *5*, 1062–1080. (b) Cozzi, F.; Annunziata, R.; Benaglia, M.; Cinquini, M.; Raimondi, L.; Baldridge, K. K.; Siegel, J. S. *Org. Biomol. Chem.* **2003**, *1*, 157–162. (c) Cozzi, F.; Cinquini, M.; Annunciata, R.; Dwyer, T.; Siegel, J. S. *J. Am. Chem. Soc.* **1992**, *114*, 5729–5733. (d) Rashkin, M. J.; Waters, M. L. *J. Am. Chem. Soc.* **2002**, *124*, 1860–1861.

Published on Web 01/14/2010 DOI: 10.1021/jo902013v

component resulting from two approaching π electron clouds.[4] In contrast, the effect of the substituents on cation$-\pi$[5] or CH$-\pi$[6] interactions follows an opposite trend and the magnitude of these interactions usually increases as attaching electron-donating substituents. The substituents also have an influence in the geometry of the stacking motifs. Thus, electron-withdrawing groups decrease the π electron density and facilitate a face-to-face geometry as a result of the diminution of the π electron repulsion while increasing the π electron density favors an offset or T-shaped staking, hence maximizing attractive $\pi-\sigma$ interactions.

The recent growth of the field of organic electronics has aroused a renewed interest on the understanding of weak intermolecular interactions involving π-conjugated molecules, a prerequisite to induce their self-assembly into one-dimensional nanostructures. Face-to-face π-stacks of extended aromatics with the π-surfaces located within van der Waals distances have emerged as promising nanowires and are among the best performing organic semiconductors.[7] In addition, self-assembled arrays formed in solution have been successfully transferred onto solid supports,[8] resulting in highly oriented films with important implications in the development of molecule-based electronic devices.

In this context we became interested on the electron-rich 10,15-dihydro-5*H*-diindolo[3,2-*a*:3′,2′-*c*]carbazole (triindole). This molecule can be formally considered as an extended π-system in which three carbazole units share an aromatic ring. Triindole-based single crystalline or liquid crystalline materials have been found to exhibit high charge mobilities (up to $\mu = 0.4$ cm^2 V^{-1} s^{-1}) since they combine the good hole transport properties characteristic of carbazoles with highly ordered columnar supramolecular arrangements.[9] Triindole derivatives have also been recognized as promising precursors for the construction of triazafulleres,[10] C_3-symmetrical tripods,[11] or optically active materials in electronic devices.[12] In addition, we have recently reported on the stacking properties in solution of a number of hexaarylalkynyl triindoles.[13]

In this paper we describe the synthesis and self-assembly of a series of N-alkyl-substituted hexaaryltriindoles functionalized with peripheral substituents of different electronic nature. The electronic communication of the terminal groups with the central electron-rich triindole core has been confirmed by optical spectroscopy and cyclic voltammetry. While these molecules exist as monomers in $CDCl_3$ solutions, we have induced aggregation by adding polar solvents and therefore facilitating the appearance of solvophobic forces in some of these derivatives. These molecules pack in the solid state as dimeric assemblies as has been determined by X-ray analysis of single crystals of two different derivatives showing opposed aggregation behavior in solution. In fact, crystallographic packing evidences the cooperative contribution of a number of CH$-\pi$ interactions between the α-methylenic group of the N-alkyl chains and the external rings of the triindole core.

Results and Discussion

Synthesis of Hexaaryltriindoles. The synthesis of the new hexasubstituted triindoles starts from known[13] symmetrical *N*-dodecyl hexabromotriindole **1**. The presence of six bromine atoms at strategic positions in this derivative offers varied opportunities for a versatile functionalization applying different cross-coupling methodologies.

Six-fold Suzuki coupling of **1** with a variety of phenylboronic acids in the presence of $Pd(PPh_3)_4$ and 2 M aqueous K_2CO_3, using THF as solvent, readily gave **2a**−**e** (61−89%), displaying six aryl groups surrounding a triindole nucleus in good yield. The presence of the long alkyl chain on the nitrogen functionalities confers to the molecule enhanced solubility and stability and therefore facilitates the Suzuki coupling reactions (Scheme 1).

Electronic Properties. The electronic properties of this series of triindoles have been investigated by UV−vis absorption and fluorescence spectroscopy (Table 1, Figure 1) and cyclic voltammetry (Figure 2 and in the Supporting Information Figures S1−S5).

With the exception of **2e** whose fluorescence is efficiently quenched due to the presence of the nitro substituents,[14] the triindoles are well fluorescent with compound **2a** displaying an especially high fluorescence quantum yield of 0.81 in solution.[15] The large Stokes shifts between 78 and 127 nm observed for all triindole derivatives are the consequence of both the nuclear reorganization taking place after irradiation and prior to emission as a result of electronic redistribution

(4) (a) Hunter, C. A.; Sanders, J. K. M. *J. Am. Chem. Soc.* **1990**, *112*, 5525–5534. (b) Cozzi, F.; Siegel, J. *Pure Appl. Chem.* **1995**, *67*, 683–689.

(5) (a) Hunter, C. A.; Low, C. M. R.; Rotger, C.; Vinter, J. G.; Zonta, C. *Proc. Natl. Acad. Sci. U.S.A.* **2002**, *99*, 4873–4876. (b) Ma, J. C.; Dougherty, D. A. *Chem. Rev.* **1997**, *97*, 1303–1324.

(6) Hirota, M.; Sakaibara, K.; Suezaea, H.; Yuzuri, H.; Ankai, E.; Nishio, M. *J. Phys. Org. Chem.* **2000**, *13*, 620–623.

(7) (a) Warman, J. M.; de Haas, P. M.; Dicker, G.; Grozema, F. C.; Piris, J.; Debije, M. G. *Chem. Mater.* **2004**, *16*, 4600–4609. (b) Smits, E. C. P.; Mathijssen, S. G. J.; van Hal, P. A.; Estalles, S.; Geuns, T. C. T.; Mutsaers, K. A. H. A.; Cantatore, E.; Wondergem, H. J.; Werzer, O.; Resel, R.; Kemerink, M.; Kirchmeyer, S.; Muzafarov, A. M.; Ponomarenko, S. A.; de Boer, B.; Blom, P. W. M.; de Leeuw, D. M. *Nature* **2008**, *455*, 956–959. (c) Percec, V.; Glodde, M.; Bera, T. K.; Miura, Y.; Shiyanovskaya, I.; Singer, K. D.; Balagurusamy, V. K.; Heiney, P. *J. Am. Chem. Soc.* **2006**, *128*, 10700–10701. (d) Xiao, S.; Myers, M.; Miao, Q.; Sanaur, S.; Pang, K.; Steigerwald, M. L.; Nuckolls, C. *Angew. Chem., Int. Ed.* **2005**, *44*, 7390–7394. (e) Zang, L.; Che, Y.; Moore, J. S. *Acc. Chem. Res.* **2008**, *41*, 1596–1608. (f) Anthony, J. E.; Brooks, J. S.; Eaton, D. L.; Parkin, S. R. *J. Am. Chem. Soc.* **2001**, *123*, 9482–9483. (g) Sokolov, A.; Friscic, T.; MacGillivray, L. R. *J. Am. Chem. Soc.* **2006**, *128*, 2806–2807.

(8) (a) Jonkheijm, P.; Hoeben, F. J. M.; Kleppinger, R.; van Herrikhuyzen, J.; Schenning, A. P. H. J.; Meijer, E. W. *J. Am. Chem. Soc.* **2003**, *125*, 15941–19949. (b) Chen, Z.; Stepanenko, V.; Dehm, V.; Prins, P.; Siebbeles, L. D. A.; Seibt, J.; Marquetand, P.; Engel, V.; Würthner, F. *Chem.—Eur. J.* **2007**, *13*, 436–449. (c) Wang, J.-Y.; Yan, J.; Li, Z.; Han, J.-M.; Ma, Y.; Bian, J.; Pei, J. *Chem.—Eur. J.* **2008**, *14*, 7760–7764. (d) Nguyen, T.-Q.; Martel, R.; Bushey, M.; Avouiris, P.; Carlsen, A.; Nuckolls, C.; Brus, L. *Phys. Chem. Chem. Phys.* **2007**, *9*, 1515–1532.

(9) (a) Talarico, M.; Termine, R.; García-Frutos, E. M.; Omenat, A.; Serrano, J. L.; Gómez-Lor, B.; Golemme, A. *Chem. Mater.* **2008**, *20*, 6589–6591. (b) García-Frutos, E. M.; Gutierrez-Puebla, E.; Monge, M. A.; Ramírez, R.; de Andrés, P.; de Andrés, A.; Ramírez, R.; Gómez-Lor, B. *Org. Electron.* **2009**, *10*, 643–652.

(10) Otero, G.; Biddau, G.; Sánchez-Sánchez, C.; Caillard, R.; López, M. F.; Rogero, C.; Palomares, F. J.; Cabello, N.; Basanta, M. A.; Ortega, J.; Méndez, J.; Echavarren, A. M.; Pérez, R.; Gómez-Lor, B.; Martín-Gago, J. A. *Nature* **2008**, *454*, 865–869.

(11) García-Frutos, E. M.; Gómez-Lor, B.; Monge, A.; Gutiérrez-Puebla, E.; Alkorta, I.; Elguero, J. *Chem.—Eur. J.* **2008**, *14*, 8555–8561.

(12) (a) Lai, W.-Y.; He, Q.-Y.; Zhu, R.; Chen, Q.-Q.; Huang, W. *Adv. Funct. Mater.* **2008**, *18*, 265–276. (b) Levermore, P. A.; Xia, R.; Lai, W.; Wang, X. H.; Huang, W.; Bradley, D. D. C. *J. Phys. D: Appl. Phys.* **2007**, *40*, 1896–1901.

(13) García-Frutos, E. M.; Gómez-Lor, B. *J. Am. Chem. Soc.* **2008**, *190*, 9173–9177.

(14) Valeur, B., *Molecular Fluorescence*; Viley-VCH: Weinheim, Germany, 2002.

(15) Quinine sulfate has been used as fluorescence standart, see: Velapoldi, R. A. In *Advances in Standards and Methodology in Spectrophotometry*; Burgess, C., Mielenz, K. D., Eds.; Elsevier Science Publishers: Amsterdam, The Netherlands, 1987; pp 175−193.

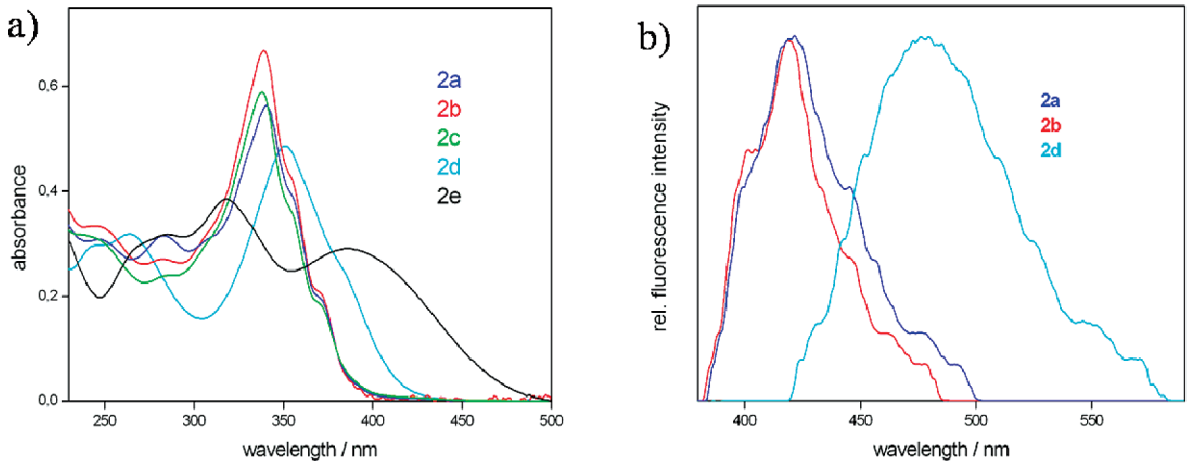

FIGURE 1. (a) UV−vis absorption spectra of **2a**−**e** in CH_2Cl_2, $c = 5 \times 10^{-6}$ mol L^{-1}; (b) normalized fluorescence spectra of **2a**, **2b**, and **2d**, $c = 5 \times 10^{-6}$ mol L^{-1}; excitation at 350 nm; **2c** omitted for clarity.

SCHEME 1. Synthesis of Hexaaryltriindoles 2a−e

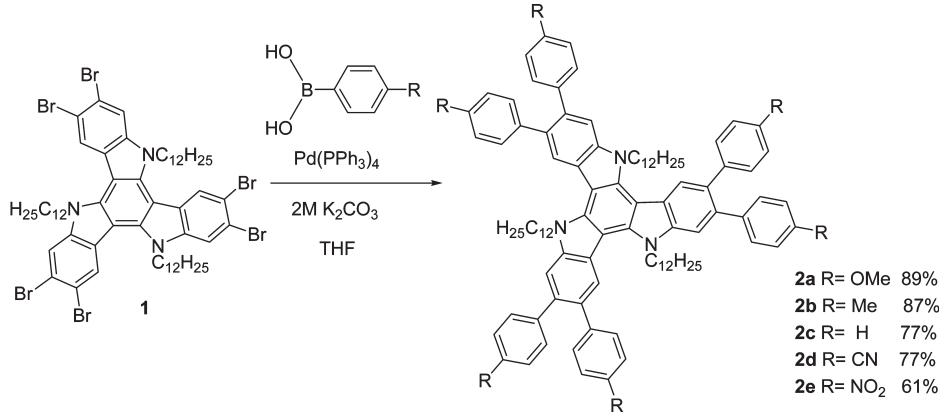

TABLE 1. UV−Vis and Fluorescence Spectroscopic Properties of 2a−e in CH_2Cl_2

compd	$\lambda_{max,abs}$/ nm	log (ε)	$\lambda_{max,em}$/nm	Φ_f
2a	341	5.055	419	0.81
2b	339	5.133	419	0.73
2c	338	5.074	422	0.31
2d	351	4.989	478	0.12
2e	386	4.777		

and the conformational changes in the biphenyl fragments (planarization) upon excitation.[16]

The influence of the peripheral groups on the electronic properties of the differently substituted hexaaryltriindoles is clearly reflected in their spectroscopic behavior. While absorption and emission spectra of **2a**−**c** are almost identical, absorption and emission spectra of **2d**−**e** show distinctive features of charge transfer: high extinction coefficients

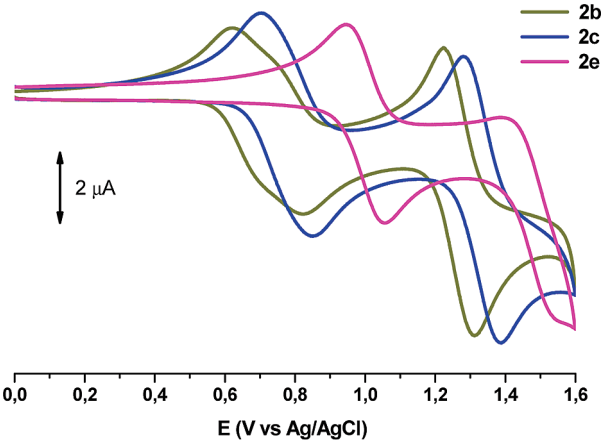

FIGURE 2. Cyclic voltammogram of **2b**, **2c**, and **2e** at $c = 10^{-3}$ mol L^{-1} in CH_2Cl_2 and 0.1 M tetra-*n*-butylammonium hexafluorophosphate ($TBAPF_6$) at a scan rate of 100 mV/s, using a Pt working electrode.

in the order of 10^5 M^{-1} cm^{-1}, bathochromic shifts of the absorption and emission maxima ($\Delta\lambda_{max,abs\ (2b-e)} = 47$ nm, $\Delta\lambda_{max,em\ (2b-e)} = 59$ nm) accompanied by a continuous loss of the vibronic fine structure of the respective band.[17]

(16) (a) Mank, D.; Raytchev, M.; Amthor, S.; Lambert, C.; Fiebig, T. *Chem. Phys. Lett.* **2003**, *376*, 201–206. (b) Hennrich, G.; Cavero, E.; Hanes, R. E.; Serrano, J. L. *Eur. J. Org. Chem.* **2008**, 4575–4579.

(17) The spectroscopic study of compounds **2a**−**d** was conducted at different concentrations (5×10^{-5} to 10^{-7} mol/L) and different solvents (MeOH and CH_2Cl_2) to determine if some aggregation behavior can be observed by optical spectroscopy. No aggregation is observed in the submillimolar concentration range required for spectroscopy.

Compounds **2d**−**e** represent π systems with a marked octopolar (nondipolar) character,[18] in which the charge-transfer process is predominantly occurring between the electron-rich triindole core and the peripheral substituents.

The increase of the electron density in the π system upon attaching electron-donating (**2a**,**b**) substituents has been demonstrated by cyclic voltammetry. Compounds **2a**−**e** can be easily oxidized to stable radical cations[19] and higher cationic charged species in the accessible potential window of the solvent. The oxidizing potentials are markedly influenced by the electronic nature of the substituents reflecting the electronic communication of the external substituents with the central electron-rich triindole core. Thus, attaching electron-donating groups (**2a**,**b**) results in an increase of the electron density in the π system and in consequence in a shift of the oxidation potentials to lower values. In contrast, upon attaching peripheral electron-withdrawing groups (**2d**,**e**), the oxidation potential shifts anodically with increasing the acceptor character of the substituents (Figure 2; also see the Supporting Information).

Self-Assembly Behavior in Solution. Disk-shaped molecules and related shape-persistent macrocycles have a strong tendency to exhibit aggregation in solution forming either dimeric[20] structures or extended stacks.[21] The aggregation behavior of this family of molecules was studied by concentration-dependent ^{1}H NMR spectroscopy. Chemical upfield shifts of the aromatic signals upon increasing the concentration in nuclear magnetic resonance spectroscopy have been well documented as a signature of aromatic interactions. When two or more aromatic units come into close vicinity of each other, the nuclei of one molecule are affected by the ring-current magnetic anisotropy of the other, resulting in resonance shifting.

The ^{1}H NMR spectra of **2a**−**e** show no concentration-dependent chemical shifting indicating that these molecules only exist as monomers in chloroform solutions. However, we attempted to drive self-assembly by adding certain amounts of polar solvents. Since the compounds are not soluble in neat CD_3OD and CD_3COCD_3 at the NMR concentration level, the NMR samples were prepared by adding the maximum volume of polar solvents to chloroform solutions (prior to precipitation). The ^{1}H NMR spectra of **2a**−**c** recorded in mixed solvent systems $CDCl_3/CD_3COCD_3$ (7:3) and $CDCl_3/CD_3OD$ (7:3) are notably sensitive to concentration changes with signals of the aromatic protons moving upfield as the concentration increased from 10^{-3} to 10^{-2} M . A pronounced upfield effect can also be observed for the α-CH_2 proton signals of the *N*-dodecyl chains. In contrast, ^{1}H NMR spectra of **2d**,**e** are not sensitive to concentration changes (Figure S13, Supporting Information).

To determine the average size of the aggregates, we have performed DOSY (diffusion-ordered spectroscopy) experiments in $CDCl_3/CD_3OD$ (7:3) on two different derivatives, one that aggregates in this solvent mixture (**2a**) and another that does not associate (**2d**) as indicated by the insensitivity of its NMR signals to concentration changes.

This NMR technique provides information of the translational diffusion coefficient of the molecular species in solution and is being increasingly employed to gain insight into the nature of supramolecular structures in solution.[22] The diffusion coefficients (D) can be related to the hydrodynamic radius (R) of the species in solution by the Stokes−Einstein equation: $D = k_BT/(6\pi\eta R)$, where T is the temperature, η is the viscosity of the solvent, R is the hydrodynamic radius of the molecule or assembly, and k_B is the Boltzmann constant. Thus, the size of the corresponding species can be compared based on their diffusion coefficients when the other parameters are identical.

The DOSY spectra of **2a** and **2d** were recorded in $CDCl_3/CD_3OD$ (7:3) at a 1.5×10^{-2} M concentration. The two-dimensional spectra shown in Figure 3 correlate ^{1}H NMR chemical shifts with the diffusion coefficient for **2a** and **2d**, respectively. For **2a** only a single apparent diffusion coefficient was observed since there is a fast exchange between the monomer and the aggregated species. The apparent diffusion coefficient found for compound **2a** is very similar to that of monomeric **2d** (approximately 2.9×10^{-10} m^2 s^{-1}) used as reference. This observation suggests the preference toward dimerization over extended aggregation. Due to the extended shape of these molecules dimers are expected to have only a slightly larger hydrodynamic volume than monomers.[22a,23] In contrast highly aggregated species would have much larger R values than monomers and consequently when comparing DOSY NMR spectra of **2a** with **2d** an important decrease of the D value would be expected.

Further evidence of the tendency of these molecules to dimerize was obtained from the MALDI-TOF MS spectra of **2a** in which a major peak for the monomer and a peak of lower intensity for the dimer can be detected, and no higher aggregates are observed (Supporting Information, Figure S6).

The relative tendency of compounds **2a**−**c** to aggregate in solution was therefore quantitatively investigated assuming a predominant monomer−dimer equilibrium.[24] The association constants (K_a) were determined by least-squares curve fitting[25]

(18) (a) Zyss, J.; Ledoux, I. *Chem. Rev.* **1994**, *94*, 77–105. (b) Beljonne, D.; Wensleers, W.; Zojer, E.; Shuai, Z.; Vogel, H.; Pond, S. J. K.; Perry, J. W.; Marder, S. R.; Bredas, J.-L. *Adv. Funct. Mater.* **2002**, *12*, 631–641.

(19) Gómez-Lor, B.; Hennrich, G.; Alonso, B.; Monge, A.; Gutierrez-Puebla, E.; Echavarren, A. M. *Angew. Chem., Int. Ed.* **2006**, *45*, 4491–4494.

(20) (a) Wu, J.; Fechtenkötter, A.; Gauss, J.; Watson, M. D.; Kastler, M.; Fechtenkötter, C.; Wagner, M.; Müllen, K. *J. Am. Chem. Soc.* **2004**, *126*, 11311–11321. (b) de Frutos, O.; Granier, T.; Gómez-Lor, B.; Jiménez-Barbero, J.; Monge, A.; Gutierrez-Puebla, E.; Echavarren, A. M. *Chem.—Eur. J.* **2002**, *8*, 2879–2890. (c) Shetty, A. S.; Zhang, J.; Moore, J. S. *J. Am. Chem. Soc.* **1996**, *118*, 1019–1027. (d) Klyatskaya, S.; Dingenouts, N.; Rosenauer, C.; Müller, B.; Höger, S. *J. Am. Chem. Soc.* **1996**, *128*, 3150–3151.

(21) (a) Kastler, M.; Pisula, W.; Wasserfallen, D.; Pakula, T.; Müllen, K. *J. Am. Chem. Soc.* **2005**, *127*, 4286–4296. (b) Klyatskaya, S.; Dingenouts, N.; Rosenauer, C.; Müller, B.; Höger, S. *J. Am. Chem. Soc.* **1996**, *128*, 3150–3151. (c) Tobe, Y.; Utsumi, N.; Kawabata, K.; Nagano, A.; Adachi, K.; Araki, S.; Sonoda, M.; Hirose, K.; Naemura, K. *J. Am. Chem. Soc.* **2002**, *124*, 5350–5364.

(22) (a) Chen, Z.; Stepanenko, V.; Dehm, V.; Prins, P.; Siebbeles, L. D. A.; Seibt, J.; Marquetand, P.; Engel, V.; Würthner, F. *Chem.—Eur. J.* **2007**, *13*, 436–449. (b) Giuseppone, N.; Schmitt, J.-L.; Allouche, L.; Lehn, J.-M. *Angew. Chem., Int. Ed.* **2008**, *120*, 2267–2271. (c) For a review on DOSY experiments on supramolecular chemistry see: Cohen, Y.; Avram, L.; Frish, L. *Angew. Chem., Int. Ed.* **2005**, *44*, 520–554.

(23) (a) Dobrawa, M.; Lysetska, M.; Ballester, P.; Grüne, F.; Würthner, F. *Macromolecules* **2005**, *38*, 1315–1325. (b) Viel, S.; Mannina, L.; Segre, A. *Tetraheron Lett.* **2002**, *43*, 2515–2519.

(24) Although definitive correlations between the behavior in solution and in solid state cannot be driven the aggregation motif observed in the solid state further supports the tendence of these molecules to dimerize.

(25) The least-squares curve fitting to the theoretical equation:

$$\delta = \delta_m + (\delta_a - \delta_m)\left(1 + \frac{1 - \sqrt{8KC_t + 1}}{4KC_t}\right)$$

where C_t is the total substrate concentration and δ the observed ^{1}H NMR chemical shifts, was carried out in order to determine the association constant K_a, and the chemical shifts of the monomer δ_m and the dimer δ_d. Martin, R. B. *Chem. Rev.* **1996**, *96*, 3043–3064.

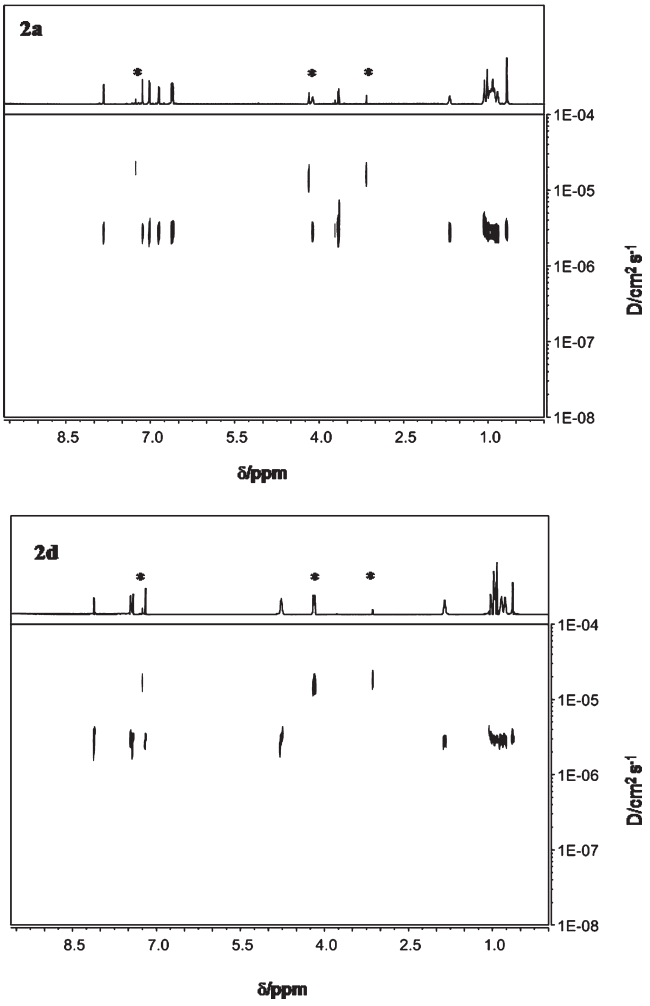

FIGURE 3. DOSY NMR spectra of **2a** and **2d** at $c = 1.5 \times 10^{-2}$ mol L^{-1} in $CDCl_3/CD_3OD$ (7:3). The signals of chloroform and methanol are marked with an asterisk. Chloroform and methanol molecules appear at significantly larger diffusion coefficient as expected from their much smaller size.

of the concentration-dependent NMR chemical shifts for triindole hydrogens in positions meta to the nitrogens[26] since these are the lowest field resonance and are clearly differentiated from the rest of the signals (Figure 4).

The association constants calculated were found to range from 68 to 223 M^{-1} in $CDCl_3$/ CD_3COCD_3 (7:3) and from 247 to 421 M^{-1} in $CDCl_3/CD_3OD$ (7:3) (Table 2, see Supporting Information).

From the value of the association constants it can be concluded that increasing the electron-donating character of the terminal *p*-phenyl substituents leads to self-association while attaching electron-withdrawing groups inhibits aggregation as previously observed in related phenylethynyl derivatives.[13] Derivatives functionalized with electron-withdrawing groups have a marked octopolar character as a result of a push−pull effect occurring between the electron-rich core and the peripheral substituents. Presumably, increasing the polarity of the stacking surfaces diminishes their mutual repulsion from the

(26) Unequivocal ^1H assignments were made on the basis of HSQC and HMBC and experiments performed on compound **2a**.

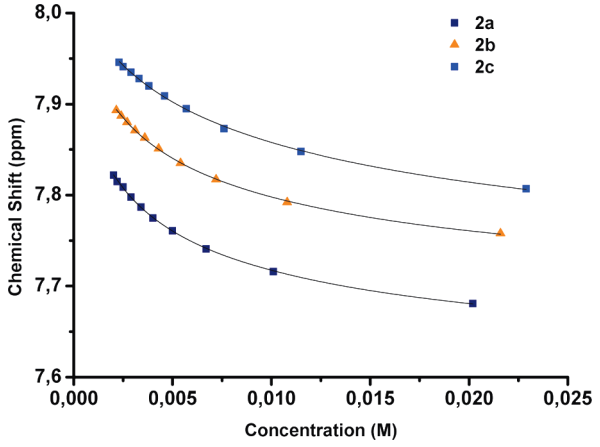

FIGURE 4. Concentration dependence of ^1H NMR chemical shifts for the lowest field singlets of **2a**−**c** in $CDCl_3/CD_3COCD_3$ (7:3).

TABLE 2. Association Constants and Chemical Shifts Calculated for the Lowest Field Resonance for 2a−c

	$CDCl_3/CD_3COCD_3$ (7:3)			$CDCl_3/CD_3OD$ (7:3)		
compd	K_a (M^{-1}) [a]	δ_d [b]	δ_m [c]	K_a (M^{-1}) [a]	δ_d [b]	δ_m [c]
2a	223 ± 26	7.57	7.97	421 ± 140	7.69	8.21
2b	161 ± 20	7.64	8.01	286 ± 120	7.73	8.15
2c	68 ± 9	7.64	8.02	247 ± 81	7.77	8.23

[a]Determined at room temperature on the basis of a dimerization model. [b]Calculated chemical shifts for the dimer. [c]Calculated chemical shifts for the monomer.

surrounding solvent and therefore decreases their stacking propensity.

However, the involvement of other additional forces in the aggregation process cannot be discarded. In particular, the clear upfield shift of the α-CH_2 proton signals of the *N*-dodecyl chains upon increasing the concentration would be in agreement with the contribution of CH−π interactions in these aggregation processes. In this platform, the occurrence of CH−π interactions is facilitated by the electron-withdrawing effect of the nitrogen on the CH component and is expected to be favored upon increasing the electron density of the aromatic partner explaining the observed stacking trends.[27]

Crystal Structure. To obtain deeper understandings of the intermolecular interactions taking place between these derivatives we have grown crystals of two triindole derivatives (**2c** and **2d**) showing opposed aggregation trends, mimicking the conditions found in solution to induce self-assembly.[28] Compound **2c** forms stable crystals by slow evaporation of a CH_2Cl_2:acetone (7:3) solvent mixture. Crystals of compound **2d** were obtained from slow evaporation of a CH_2Cl_2:EtOAc (7:3) solvent mixture, but they readily decompose out of the crystallization mixture presumably due to the loss of the cocrystallized solvent molecules. Therefore the crystals were soaked in oil immediately after extraction from the solvent

(27) Nishio, M.; Hirota, M.; Umezawa, Y. *The CH/π interaction. Evidence, Nature and Consequences*; Wiley-VCH: New York, 1998.

(28) It has been found that the study of intermolecular aggregates by solution NMR can provide some insights into the structure of crystalline materials, offering useful hints about the crystal nucleation. Spitaleri, A.; Hunter, C. A.; McCabe, J. F.; Packer, M. J.; Cockroft, S. L. *CrystEngComm* **2004**, *6*, 489–493.

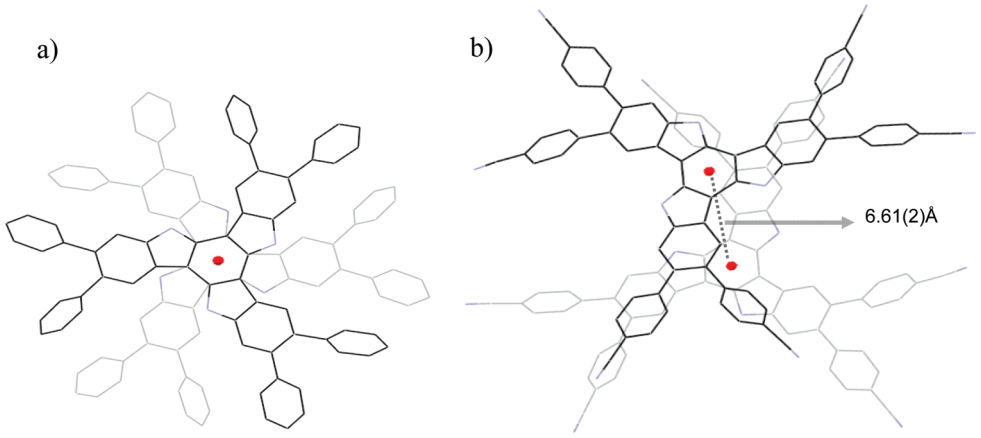

FIGURE 5. View of the dimeric packing perpendicular to the molecular mean plane of **2c** (left) and **2d** (right).

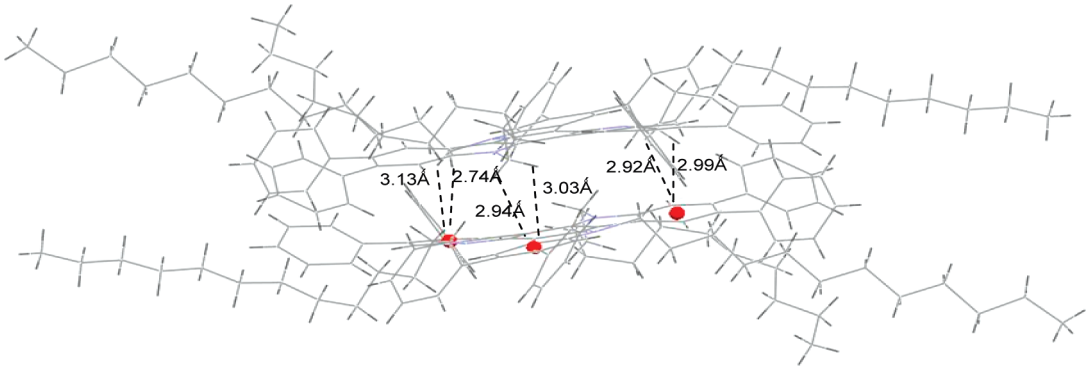

FIGURE 6. CH$-\pi$ interactions stabilizing the dimeric motif of **2c**. The dimer is stabilized by six additional interactions (not shown) related by an inversion center to those depicted.

crystallization mixture, and cooled in a nitrogen stream where data collection was performed at -100 °C.[29]

Although correlations between the behavior in solution and in solid state must be considered with caution, comparisons of the molecular packing in these two structures allow us to see additional interesting features. Molecules of **2c** pack in the crystal forming dimeric aggregates (Figure 5a), with the triindole units situated at 3.65(2) Å (average distance between centroids of the central aromatic rings of the platforms). Within the dimers, the molecules are oriented face-to-face in an alternate arrangement, one molecule rotated 180° with respect to the next molecular unit, being the central aromatic rings are perfectly superimposable. In contrast, the closest molecules of **2d** in the crystal lattice are found slipped in parallel planes (distance between mean planes: 3.82(2) Å), shifted 6.61(2) Å (distance between the centroids of the central aromatic rings) (Figure 5b).

The effect of the substituents on the geometry of the stacking in the solid follows again an opposite behavior to that expected for an aggregation ruled exclusively by π interactions, predicting that an increase of the π-electron density favors an offset or T-shaped staking by maximizing attractive $\pi-\sigma$ interactions, while decreasing π electron density facilitates the face-to-face geometry as a result of the diminution of π electron repulsion. The stacking motifs observed cannot be rationalized just in terms of solvophobic forces and point to the contribution of an additional component inherent to the molecular structure in the aggregation. In fact close inspection of both dimeric structures shows that a number of cooperative CH/π interactions are playing an important role in the formation of these aggregates. Short contacts between the hydrogens on the methylenic group α to the nitrogens and the external aromatic rings of the triindole platform are observed in the dimeric structure of **2c** and **2d** (12 interactions: Figure 6; four interactions: Figure S15, Supporting Information).

Conclusion

In conclusion, we have described the self-assembly properties in solution and in solid state of a series of differently substituted *N*-alkyl hexaaryltriindoles. Self-assembly in solution could be induced by adding polar solvents. A study of the electronic character of the triindole π-systems on their self-association behavior indicates that in solution increasing the electron-donating character of the terminal *p*-phenyl substituents facilitates self-association, while electron-withdrawing groups inhibit aggregation. X-ray crystal structure analysis reveals further details on the nature of the aggregates in the solid state. While molecules of hexaphenyltriindole **2c** pack in the crystals as dimeric aggregates, with a

(29) Both crystals diffract poorly and a large portion of measured reflexions had negative intensities and were eliminated. Because of this the completeness percentages are low in both crystals. In addition the long alkylic chains are highly disordered and had to be refined with restriction. This is a common feature of crystals of organic compounds with long alkyl chains. In spite of these problems, the central core of the molecules could be perfectly determined with accuracy.

perfect face-to-face stacking arrangement, withdrawing electron density of the system by attaching six peripheral cyano functional groups (**2d**) results in an offset geometry of the aggregates. The effect of the substituents in the strength and geometry of this interaction cannot be explained in terms of the decrease of a repulsive component resulting from interaction of the π-clouds as usually invoked in $\pi-\pi$ interactions. However, it can be rationalized considering an important contribution of several cooperative CH$-\pi$ interactions between CH moieties of the alkylic chains and the external rings on the triindole platform.

The results presented here highlight the importance of evaluating the delicate balance between all the possible different interactions when designing new superstructures involving aromatics.

Experimental Section

Typical Coupling Procedure: Preparation of 2,3,7,8,12,13-Hexakis(*p*-methoxyphenyl)-5,10,15-tris(dodecyl)-10,15-dihydro-5*H*-diindolo[3,2-*a*:3′,2′-*c*]carbazole (2a). A mixture of **1** (100 mg, 0.075 mmol), $Pd(PPh_3)_4$ (43 mg, 0.037 mmol), and 4-methoxyphenylboronic acid (130 mg, 0.85 mmol) was degassed. Then 0.5 mL of 2 M aqueous K_2CO_3 and 4 mL of THF was added. The mixture was heated at 90 °C for 4 days under nitrogen. The orange suspension was partitioned between H_2O and CH_2Cl_2, then dried ($MgSO_4$). The solvent was evaporated and the residue was precipitated with CH_2Cl_2 and acetonitrile and filtered to give a yellow solid **2a** (101 mg, 89%): mp 136−138 °C; ^{1}H NMR (200 MHz, $CDCl_3$) δ 8.27 (s, 3H), 7.57 (s, 3H), 7.25−7.19 (m, 12H), 6.84 (d, J = 8.7 Hz, 6H), 6.83 (d, J = 8.5 Hz, 6H), 4.92 (m, 6H), 3.83 (s, 18H), 2.07 (m, 6H), 1.21 (m, 54H), 0.86 (t, J = 6.7 Hz, 9H); ^{13}C NMR (50 MHz, $CDCl_3$) δ 158.1, 157.9, 140.3, 139.4, 135.5, 135.4, 135.0, 132.6, 131.3, 123.4, 122.3, 113.3, 111.5, 102.8, 55.1, 47.0, 31.9, 30.4, 29.6, 29.3, 26.8, 22.7, 14.1; UV (CH_2Cl_2, 25 °C) λ_{max} (log ε) 341 (5.05); MALDI-TOF MS m/z 1487 (M^+ + 1); HRMS (MALDI-TOF) calcd for $C_{102}H_{123}N_3O_6$ 1485.94064, found 1485.94543.

Acknowledgment. Financial support from the MEC (CTQ2007-65683/BQU, is gratefully acknowledged). E.M. G.-F. thanks the Consejo Superior de Investigaciones Científicas (Program I3P) for a posdoctoral contract. We are grateful to Dr. Manuel Martin (Universidad de Santiago de Compostela) for assistance with DOSY NMR experiments.

Supporting Information Available: Experimental procedures, synthesis, characterization, and copies of ^{1}H NMR and ^{13}C NMR spectra of all new compounds, MALDI-TOF MS spectrum of **2a**, DOSY-NMR experiment details, tabulated ^{1}H NMR data, calculated association constants, copies of ^{1}H NMR experiments at variable concentrations of **2a** and **2d** in $CDCl_3$/CD_3COCD_3 (7/3), and X-ray data of **2c** and **2d**. This material is available free of charge via the Internet at http://pubs.acs.org.